Windage measurements in a rotor stator cavity with rotor mounted protrusions and bolts

Article (Published Version)

Proceedings of ASME Turbo Expo 2012
GT2012
June 11-15, 2012, Copenhagen, Denmark

GT2012 69385

Windage Measurements in a Rotor Stator Cavity with Rotor Mounted Protrusions and Bolts

C. A. Long, A. L. Miles

Thermo-Fluid Mechanics Research Centre
School of Engineering & Design
University of Sussex
Brighton, BN1 9QT
U.K.

D. D. Coren

Department of Mechanical Engineering
Imperial College London
South Kensington
London, SW7 2AZ
U.K.

ABSTRACT

This paper reports an experimental investigation of the windage associated with enclosed rotor-stator systems with superposed throughflow, as commonly found in gas turbine engines. The term windage is often used to describe the viscous heating that arises from the interaction of surfaces and fluids in rotating disc systems. Since the presence of circumferentially discreet geometric features strongly alters the magnitude of Windage measured, the physical mechanisms collectively referred to as windage in this paper are separately described as part of the discussion of results.

Tests have been carried out to measure windage directly in the form of shaft torque and also rotor surface temperature. Non-dimensional flow parameters are used to expand the relevance of the data obtained, which encompasses the ranges $0.17 \times 10^7 \leq Re_\varphi \leq 1.68 \times 10^7$ and $0.24 \times 10^5 \leq C_w \leq 1.06 \times 10^5$ which corresponds to $0.058 \leq \lambda_T \leq 0.631$. Data has been obtained for smooth disc geometry and also with rotor mounted protrusions of N = 3, 9 and 18; D = 10 mm, 13 mm and 16 mm diameter; H = 11 mm, high, hexagonal bolt shaped protrusions. Bi-hexagonal (twelve sided) bolts of D = 13 mm effective diameter, and height, H = 11mm, were also tested with conditions closely matched to the 13 mm hexagonal bolts. Finally, tests with 10 mm diameter, 6 mm deep, pockets were also carried out.

Over the range of conditions and geometries tested, increasing the number of bolts increases the moment coefficient and windage heating. At low values of turbulent flow parameter, λ_T, which correspond to rotational speeds between 8000 and 10000 rev/min, increasing the diameter of the bolts shows a clear trend for both increased windage torque and average disc temperature rise. For these conditions, there also appears to be a clear reduction in windage and temperature rise with the bi-hexagonal shaped bolts compared to the equivalent diameter hexagonal bolt form. Variation in the moment coefficient with the number and diameter of bolts is attributed to variations in form drag between the different configurations. The introduction of the recesses onto the disc has very little effect on either windage heating or moment coefficient; this is attributed to the component of windage mechanism in operation and also the relatively small size in comparison to the protrusions studied here.

This work contributes to the understanding of windage in gas turbines by introducing new low uncertainty data obtained at engine representative conditions and as such is of benefit to those involved with the design of internal air systems and disc fixtures.

1. INTRODUCTION

Increasing the efficiency of a gas turbine engine requires either a higher turbine entry temperature of the main gas flow or a reduction of internal losses. Turbine entry temperatures on modern civil engines are currently above 1600°C, and components in contact with such high temperatures quickly exceed their creep and fatigue limits. It is only possible to operate at these elevated temperatures because of internal air systems which use some of the compressor air to cool the turbine discs, blades and nozzle guide vanes. However, air used for cooling will be heated by work transfer and viscous dissipation as it flows over both rotating and stationary surfaces. This parasitic phenomenon is commonly referred to as windage. The magnitude of windage heating may also be expected to increase when features such as protrusions and pockets are fixed to the surface. More accurate windage predictions that take all windage mechanisms into consideration offer potential for improved design of the internal air system, with associated increases in thrust and efficiency.

The aim of this research is to investigate this phenomenon and gain insight into the relevant fluid dynamic mechanisms. An additional aim is to correlate windage with the flow properties and number, size and shape of these protrusions. In the work presented in this paper, this has been investigated experimentally using a pressurised rotor-stator cavity. A number of different configurations have been studied (hexagonal bolts, bi-hexagonal (12 sided) bolts and pockets) with the number and the diameter of the bolts being varied. Measurements have been made of the windage torque and rotor surface temperatures for a range of rotational speeds and superimposed mass flow rates.

This paper begins with a brief literature review and an overview of the governing flow phenomena of rotor-stator systems. This is followed with a description of the experimental test setup and methodology. The experimental results are then presented and discussed for the disc protrusion and pocket tests respectively, which is followed by the conclusions.

NOMENCLATURE

A	Frontal area of protrusion
a, b	Inner and outer radius of the disc, respectively
C_p	Specific heat capacity at constant pressure
C_D	Drag coefficient
D	Diameter of protrusion
F	Function
G = s/b	Gap ratio
H	Height of bolt
k	Thermal conductivity
$\dot{m}$	Mass flow rate to one side of the disc
M	Moment on both sides of the disc
N	Number of protrusions
p	Circumferential pitch
$R = Pr^{1/3}$	Recovery factor
r	Radial coordinate
r_b	Bolt radius
s	Axial gap between rotor and stator
$S = \beta/\beta_0$	Speed increase factor of core due to protrusions
T	Temperature
$T_{o,ad}$	Adiabatic disc temperature
V_ϕ	Tangential component of velocity in a stationary coordinate system
w	Uncertainty in independent variable x
x	Independent variable
$\beta = V_\phi/\omega r$	Core rotation factor
β^*	Value of β when $C_w = 0$
ΔT	Temperature difference
μ	Dynamic viscosity
ρ	Density
ω	Rotational speed of the disc

Subscripts

ave	Average value
ent	Entrained value
in, out	Inlet and outlet
o, p	Pertaining to a plain disc and protrusions, respectively
1,5	Pertaining to the inner and outer radial locations of the infra red sensors
∞	Value away from the disc surface

2. REVIEW OF PREVIOUS WORK

A useful starting point to understanding the flow behaviour in a rotor-stator system is the so called free disc (see Dorfman [1]). This is a solid disc of outer radius b, rotating at a speed ω in an initially stationary fluid of density ρ, and dynamic viscosity μ. Friction and the no-slip condition at the disc surface cause the flow in the disc boundary layer to be pumped radially outward, which is replaced by entrainment of flow into the boundary layer. Von Kármán's [2] solution (using a one-seventh power law for the velocity profile) for the free disc gives the entrained flow, $C_{w,ent}$ and moment coefficient, C_m as:

$$C_{w,ent} = 0.219\,Re_\phi^{0.8} \quad (1)$$

and

$$C_m = 0.146\,Re_\phi^{-0.2} \quad (2)$$

The dimensionless flow rate, C_w, rotational Reynolds number, Re_ϕ and moment coefficient, C_m are defined by:

$$C_w = \frac{\dot{m}}{\mu b} \quad (3)$$

$$Re_\phi = \frac{\rho \omega b^2}{\mu} \quad (4)$$

$$C_m = \frac{M}{1/2\,\rho\omega^2 b^5} \quad (5)$$

Where $\dot{m}$ is the mass flow *on one side of the disc* and M is the windage torque *on both sides of the disc.*

A schematic diagram of a rotor-stator cavity is shown in Figure 1. This comprises a rotating disc adjacent to a stationary disc and separated by an axial gap, s. A superimposed flow is supplied to the cavity through a central pipe of radius a, and this flows radially outward. The effect of the axial gap on the flow structure is not significant when the gap is much greater than the boundary layer thickness; which is the case in most practical applications. For no superimposed flow, $C_w = 0$ (Figure 1(a)), the flow structure comprises separate boundary layers on the rotor and stator and a central core region where there is only tangential motion with about 40% of disc speed. Flow is pumped up the rotor and moves radially inward down the stator. Daily and Nece [3] investigated this case with a fully enclosed rotor-stator test rig, showing that the gap ratio, G, influences the moment coefficient only for cases where $G \leq 0.06$. The presence of a central core region, occurring where $G > 0.06$, resulted in lower than free disc moment coefficients due to reduced boundary later velocity gradients and shear stresses.

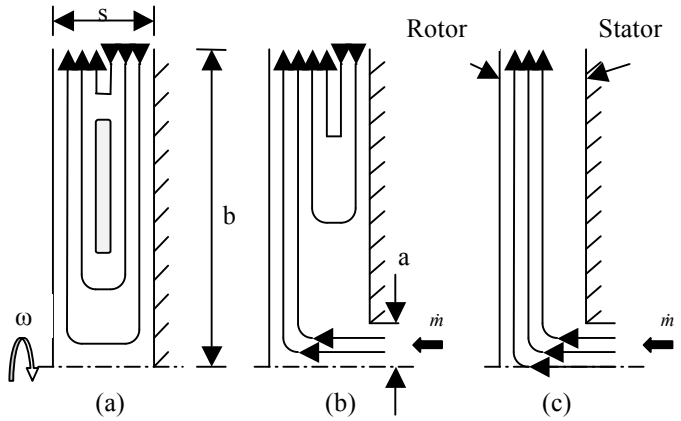

Figure 1 Schematic Diagrams of Rotor Stator Flows (after Owen and Rogers [4])
(a) $C_w = 0$, (b) $C_w < C_{w,ent}$, (c) $C_w > C_{w,ent}$,

For $C_w > 0$, increasing the superimposed flow reduces the tangential velocity of the core. For small amounts of superimposed flow (Figure 1(b)) the flow structure in the cavity is dominated by rotation; conversely for large amounts (Figure 1(c)), the flow structure is dominated by the superimposed flow. Owen and Rogers [4] developed a useful parameter to delineate these two regimes. This is the turbulent flow parameter λ_T which takes its definition from Equation 1.

$$\lambda_T = \frac{C_w}{Re_\phi^{0.8}} \qquad (6)$$

For $\lambda_T = 0.219$, the superimposed flow matches the free disc entrainment. So, the flow structure in Figure 1(b) would be appropriate for $\lambda_T < 0.219$ and that in Figure 1(c) of $\lambda_T > 0.219$. To put this into the context of gas turbine flows, values of $0.05 < \lambda_T < 0.1$ are representative of conditions in a modern high-pressure turbine disc cavity.

The core tangential velocity $V_{\phi,\infty}$ in a rotor-stator system with a peripheral shroud and with a superimposed flow was correlated by Daily, Ernst and Asbedian [5], using a modified version of the apparatus used by Daily and Nece [3], as

$$\frac{\beta}{\beta^*} = \left\{1 + 12.74 \frac{\lambda_T}{(r/b)^{13/5}}\right\}^{-1} \qquad (7)$$

where

$$\beta = V_{\phi,\infty} / \omega r \qquad (8)$$

and $\beta^*$is the value of β when $C_w = 0$ (the accepted value for turbulent flow is $\beta^* = 0.43$). These authors also measured the moment coefficient. It was found that by increasing the throughflow rate, the core tangential velocity decreased, and at the highest throughflow rates, values of C_m above those predicted by Equation (2) were measured.

The experiments of Millward and Robinson [6] involved varying the number of bolts, N, the diameter, D, circumferential pitch, p, and projected cross sectional area, A. These were attached to both the rotor, as well as on the stationary casing, at a radius r_b. For protrusions attached to the rotor, the moment coefficient obtained from the enthalpy rise was correlated by the expression:

$$C_m = 2.3 \left\{ \frac{C_w}{Re_\phi} \left(\frac{b}{r_b} \right)^3 \right\}^{\left(1.4 - \frac{r_b}{3a}\right)} \left(\frac{p}{D} \right)^{0.44} \frac{A N r_b^3}{b^5} \qquad (9)$$

They also noted that the effect on windage of bolts located towards the outer radius was very significant, whereas those located towards the inner radius had little effect. For protrusions on the stator, there was insufficient data to derive a correlation, though a recommendation was made that stator bolts contributed one third of the windage of the corresponding rotor bolts. Tests were also carried out with full and partial covering of both stator and rotor bolts. No measurable effect was found by partially covering the rotor bolts but the stator bolts showed a reduction in windage at high mass flows. Fully covered bolts however, gave similar windage to a plain disc, and in some cases a reduction in windage was actually observed.

Zimmerman et al. [7] measured the effect on shaft torque of various bolt designs. Those considered were: staged (i.e. axially stacked concentric bolts of reducing diameter), cylindrical rotor bolts, partially covered and fully covered (by an annular ring) rotor bolts. It was found that eighteen staged bolts on a disc at a radius ratio, $r_b/b = 0.75$, increased torque by a factor of 2.5, with further increases for cylindrical shaped bolts. Partially covered bolts, gave little benefit in reducing windage compared to the uncovered bolts. However, fully covered bolts, gave a significant reduction in moment coefficient compared with the uncovered bolts and a moment coefficient of approximately 25% above that of a plain disc. The effect of a superimposed flow of $C_w = 2.6 \times 10^4$ was to increase the windage by 50% for all configurations. The increased windage due to protrusions

was attributed to the superposition of three elements: form drag; boundary layer losses and pumping losses.

Gartner [8] developed a semi-empirical correlation that gives satisfactory agreement for the moment coefficient from a plain disc over a wide range of dimensionless mass flows. Gartner [9] used a momentum integral method to predict the windage torque from a single disc with protrusions. The predictions agree well with available data, providing the spacing between the bolts is not so small that wake effects become significant.

3. DESCRIPTION OF THE TEST RIG

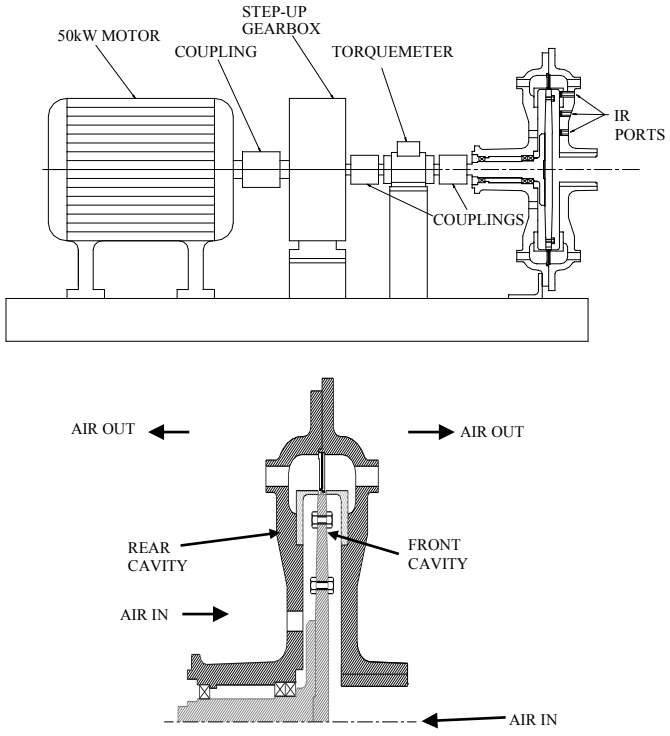

Figure 2 General Assembly of the Bolt Windage Test Rig.

Figure 2 shows a general assembly of the test rig. This consists of a shaft mounted titanium alloy disc of outer radius b = 0.225 m enclosed within a sealed steel pressure casing. The gap ratio, G, is 0.1. Around the outer rim of the disc is a labyrinth seal and a stator mounted shroud encases the cavities on either side of the disc. The disc is driven by a 50 kW motor through a 5:1 step up gearbox. Mounted between the gearbox and the disc is an in line torquemeter. The test side of the disc (labelled 'front cavity' in Figure 2) carries the majority of the instrumentation whereas the balance side (labelled 'rear cavity') has sufficient instrumentation to balance the flow conditions on both sides of the disc. A superimposed axial flow of air enters the rig centrally on the test side, flows radially outward through the cavity and leaves through the labyrinth seal at the perimeter. On the balance side, the disc driveshaft necessitates that the air enters through four inlet pipes equally spaced around the central shaft. Although the hub region flow is thus non-symmetrical, only relatively low levels of windage occur at this low radius location. The rig is not considered to have any significant flow, thermal, or pressure asymmetries attributable to this arrangement. There are four orifice plates positioned upstream and downstream of the test rig on both the test and balance side to measure the mass flow of air through the rig as well as to ensure both sides are balanced. The air is supplied at pressures of up to 7.5 bar (absolute) and mass flows of up to 0.82 kg/s by an Atlas Copco screw type compressor and treated with an Atlas Copco air conditioning unit to provide dry air in the range 15 to 25 ºC prior to delivery to the rig. At the orifice plates, differential pressure measurements are taken by Rosemount 1151 pressure transmitters. These have a maximum uncertainty of 0.075% at 1865 mbar (gauge).

The inlet and outlet air temperatures and also that at the orifice plates are measured using a number of K-Type thermocouples and platinum resistance thermometers. Infra red sensors with a sensitivity of 10 mV/°C and resolution of 0.1°C are used to measure the disc temperature at five radii on the test side: r = 0.096 m, 0.135 m, 0.154 m, 0.200 m and 0.211 m (corresponding to r/b = 0.427, 0.600, 0.684, 0.887 and 0.935 respectively). An additional single sensor is positioned at a radius of 0.200 m (r/b = 0.887) on the balance side. A shaft mounted Vibrometer TM112 in line torquemeter measures torque and rotational speed. For the torque measurement, this has a sensitivity of 25 mV/Nm and the speed signal has a sensitivity of 0.2 mV/rev/min. Signals from the thermocouples, platinum resistance thermometers, infra red sensors and torque meter are measured with two National Instruments data acquisition systems (a NI c-DAQ for the thermocouples and torquemeter and a SCXI-1001 system for the platinum resistance thermometers and infra red sensors).

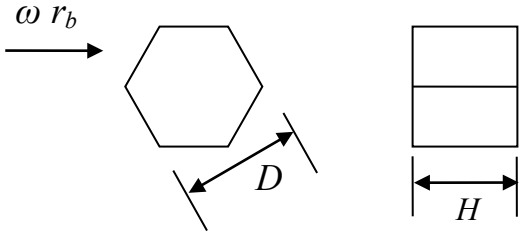

Figure 3 Orientation of Bolts with Respect to Rotation.

Following an initial series of plain disc tests, tests were carried out with N = 3, 9 and 18 and D = 10 mm, 13 mm and 16 mm, hexagonal bolts of height, H = 11 mm. These were attached, at a radius of 0.2 m, r_b/b = 0.889, to both sides of the disc surface to ensure similar conditions on either side, minimising axial conduction. The orientation of the bolts relative to the direction of rotation is shown in Figure 3. This was maintained throughout the test programme. The tests covered the range of conditions $0.17 \times 10^7 \le Re_\phi \le 1.5 \times 10^7$; $0.24 \times 10^5 \le C_w \le 1.06 \times 10^5$; $0.058 \le \lambda_T \le 0.631$. The wide range of λ_T was selected in order to obtain data encompassing the transition from rotationally to throughflow dominated flow cases, in the

interests of better understanding the relationship between flow structure and windage. Following the tests with hexagonal bolts, the test programme for D = 13 mm was repeated using bi-hexagonal (12 sided) bolts with N = 3, 9 and 18.

The rotor surface temperature measurements were acquired when the conditions were settled. This was considered to be attained when the difference between the outlet and inlet air temperatures changed by less than 0.05°C over a period of 120s. The torque due to bearing friction in the test rig depends on rotational speed and was obtained by a previous calibration (see Miles et al. [10]). This driveline torque was subtracted from all of the measured values of torque to obtain values of the windage torque, M, that are presented here. The magnitude of the driveline torque varied from 2% of the total at high rotational speeds to 20% at low values of rotational speed.

It is recognized that the enthalpy rise rate of the fluid flowing through the test section could be used to calculate a moment coefficient, however, in order to avoid uncertainty associated with estimating the heat loss through the main casing, the torque meter data has been used exclusively for the data presented here.

4. RESULTS AND DISCUSSION

Figure 4 shows the variation of $C_m Re_\phi^{0.2}$ with λ_T for the plain disc tests as well as tests with N = 9, and D = 10 mm, 13 mm and 16 mm hexagonal bolts. Also shown is Von Karman's relationship for a free disc, Equation (2), which (as do the measurements) represents the torque on both sides of the disc.

The uncertainty bars shown for the moment coefficient have been calculated using the standard technique given by:

$$w_F = \left[\left(\frac{\partial F}{\partial x_1} w_1 \right)^2 + \left(\frac{\partial F}{\partial x_2} w_2 \right)^2 + ... + \left(\frac{\partial F}{\partial x_n} w_n \right)^2 \right]^{1/2} \quad (10)$$

where F is a function of the independent variables x_1, x_2, x_3,…, x_n, w_F is the uncertainty in the result F, and w_1, w_2, w_3,….., w_n are the uncertainties in the independent variables. It is relevant to note that the uncertainty in the moment coefficient is highest at the lower values of rotational Reynolds number. This occurs because the rotational speed and the value of the measured torque are low, whilst the torquemeter uncertainty is constant.

This particular ordinate was chosen because it is a constant value for a free disc (as indicated by the solid line at $C_m Re_\phi^{0.2}$ = 0.146) and so any moment coefficient result significantly higher than this case, for a given value of λ_T, would be a direct indication of the effect of the bolts. For the rotor bolt data, the clusters of the three symbols at similar values of λ_T are results from tests carried out at similar values of Re_ϕ with the three different sizes of bolt. The plain disc results show a noticeable difference between the measured values of moment coefficient and those predicted by Equation (2). This is consistent with the results of Daily et al. [5] and can be attributed to both the design of the test rig, where the shrouding and the labyrinth seal around the perimeter are expected to generate a significant contribution to the measured torque and the assumptions of the boundary layer velocity profile made in the development of Equation (2). For cases where $\lambda_T > 0.219$, flow structures analogous to the free exist. In combination with these other contributors, moment coefficients higher than that found with the free disc case may result. For a rotor-stator system, the torque experienced by the rotor is a consequence of the tangential shear stress in the rotor as well as the stator boundary layer. Since these two boundary layers begin at different locations, and because in the presence of a rotating core they exist across dissimilar velocity gradients, a simple superposition of their effects is not equivalent to a single free disc boundary layer. Comparing the plain disc data with that for bolts attached to the rotor illustrates the significance of the effect on the moment coefficient, which can increase by a factor of three. There is evidence (LDA measurements of Coren [11] and roughness work of Kurokawa et al. [12]) to suggest that the presence of rotor bolts speeds up the core velocity. This will result in a decrease in the relative disc to core velocity and may be expected to contribute to a reduction in the skin friction drag. However, the increase in C_m shown implies that this mechanism is not significant in relation to the form drag from the protrusions, which is expected to dominate the moment coefficient over most of the range of Re_ϕ and C_w. Although the results for D = 10 mm and D = 13 mm show a small difference across the range of λ_T tested, increasing the bolt diameter to D = 16 mm does appear to show a consistent increase in moment coefficient. This is to be expected from an increase in the form drag associated with an increase in the frontal area. The effect is more noticeable at the larger values of λ_T because the contribution of the form drag to the total drag is greater here (this can be seen from the difference between the results with hexagonal bolts and those from the plain disc). The data for λ_T = 0.213 have particularly wide uncertainty bars and this is because these results were acquired at a relatively low rotational speed (3800 rev / min).

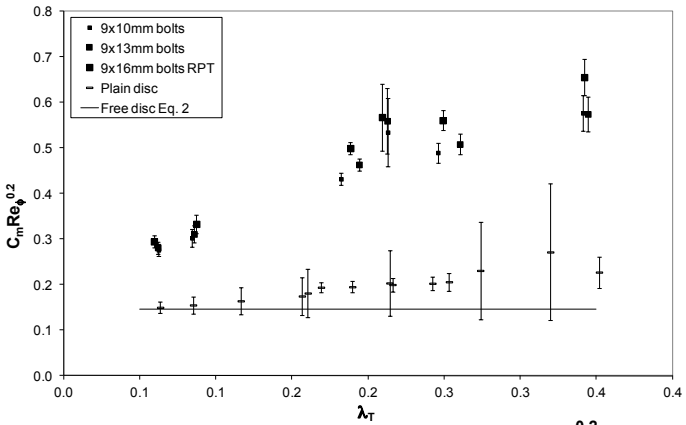

Figure 4 Hexagonal Rotor Bolts, Variation of $C_m Re_\phi^{0.2}$ with λ_T and Bolt Diameter, N = 9, D = 10mm, 13mm and 16mm.

The form drag hypothesis would, however, be expected to show a consistent increase with bolt diameter and two reasons are suggested to explain why this does not appear in the measurements:

1. The uncertainty in the moment coefficient is significant in relation to the difference in measured values of moment coefficient between the 10 mm and 13 mm bolts.
2. The flow around the bolt is complex and it can significantly affect the drag coefficient.

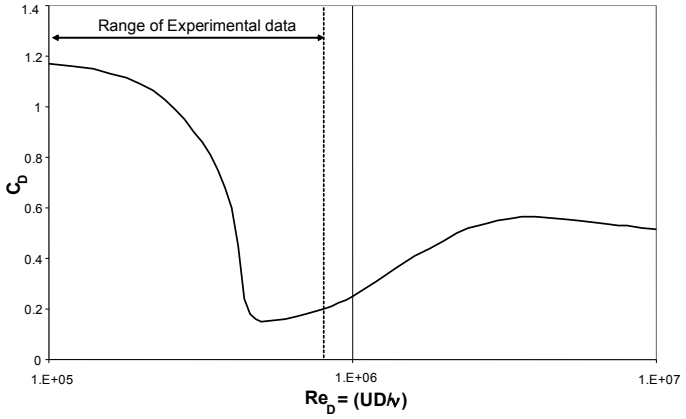

Figure 5 Variation of Drag Coefficient for a Circular Cylinder (after Schlichting [13]). For Equation (11), U = $V_{\phi,\infty}$.

Some insight into the latter can be gained from estimating a Reynolds number, Re_D, based on core velocity and using the bolt diameter as the length scale:

$$Re_D = \frac{\rho V_{\phi,\infty} D}{\mu} = \left\{(1 - S\beta_0)\frac{r_b}{b}\frac{D}{b}\right\} Re_\phi \qquad (11)$$

where $S = \beta / \beta_0$ and β_0 ($\beta_0 = f(\lambda_T)$) can be obtained from Equation (7) with $\beta^* = 0.43$. The effect of the presence of the rotor bolts on the core rotation is reflected in the value of the constant S. The relationship provided by Equation (7) was obtained from test data from plain discs and for $0.05 \leq \lambda_T \leq 0.14$. It is relevant to the data presented here because the presence of protrusions causes an increase in core rotation β. At the higher values of λ_T tested this results in values of β which are consistent with those of a plain disc at low values of λ_T. Although this topic is to be addressed in a future publication, preliminary (unpublished) measurements and also those of Coren [11] indicate that $1 < S < 3$ (depending on the values of C_w and also Re_*). For the results shown in Figure 4, the range of Re_D with S = 1 is: $10^5 < Re_D < 8 \times 10^5$. For S = 2, the corresponding range of Re_D is: $9 \times 10^4 < Re_D < 7 \times 10^5$ and for S = 3 it is $8 \times 10^4 < Re_D < 6 \times 10^5$. As shown in Figure 5, the values of drag coefficient for a circular cylinder in this range can be very sensitive to changes in Re_D. Although hexagonal bolts are likely to have different numerical values of drag coefficient the flow may be expected to behave in a similar way. For a limited range of Reynolds numbers, there is likely to be a large sensitivity of drag coefficient to the Reynolds number. The actual variation in drag coefficient with bolt Reynolds number is not expected to follow that of a cylinder, but nevertheless, the estimate suggests the data is potentially in the complex region between laminar and turbulent separations, with associated variations in wake thickness, and hence form drag.

Figure 6 shows the variation of moment coefficient C_m with number and diameter of bolts for three distinct sets of data at nominally constant values of λ_T ($\lambda_T = 0.35 \pm 4\%$, $0.19 \pm 4\%$, $0.06 \pm 6\%$). For $\lambda_T = 0.19$ and $9 \leq N \leq 18$, C_m increases with increasing bolt head diameter in a consistent trend for all three bolt head diameters. This increase is less consistent and less pronounced at the lower values of λ_T, where tangential bolt wakes are more likely to be present. This combination of C_w and Re_* corresponds to conditions where the estimated drag coefficient (albeit of an equivalent diameter cylinder) of all three bolt diameters and for $1 \leq S \leq 3$, is likely to be in the stable fully turbulent regime ($Re_D > 5 \times 10^5$), with an approximately constant value in the region of $C_D = 0.2$. For $\lambda_T = 0.06$, although the 10 mm, 13 mm and 16 mm bolt heads show a monotonic increase with N, the data for the 10 mm and 13 mm bolts are virtually indistinguishable. At this lower value of λ_T the values of Re_D are in a range where the drag coefficient is likely to be highly sensitive to small changes in bolt Reynolds number (e.g. for S = 1.5, the values of Re_D are in the range $3.0 \times 10^5 \leq Re_D \leq 4.0 \times 10^5$ as D varies from 10mm to 13mm). This suggests that the increase in form drag with frontal area is offset by a decrease in the drag coefficient. The data for $\lambda_T = 0.35$ provide a clear overall trend from increasing the bolt diameter from 10 mm to 16 mm and also the number of bolts. However the change from the 10 mm to 13 mm bolts actually shows a decrease in the moment coefficient. Although the uncertainty in the measurement for this value of λ_T, exceeds the difference in the measurement, this was a repeatable effect and a plausible explanation is again that the increase in frontal area is outweighed by a reduction in the drag coefficient.

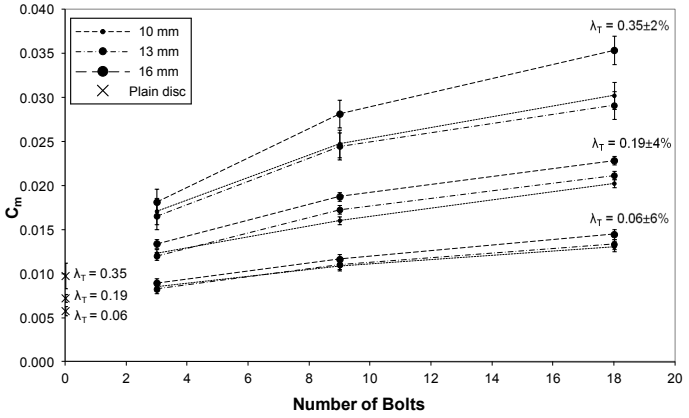

Figure 6 Hexagonal Rotor Bolts, Variation of Moment Coefficient with bolt number, N, and diameter, D = 10mm, 13mm and 16mm.

It should be noted that it is not being suggested that the hexagonal bolt heads are likely to have the same numerical variation of drag coefficient as the equivalent cylinder in pure cross flow. However, the analysis provides an illustration of the potential sensitivity of form drag to both bolt head diameter and core speed.

A reduction in moment coefficient with increasing number of bolts, as found by Millward and Robinson [6] was not observed over the range of conditions tested. This characteristic, sometimes referred to as shadowing, results from the case where bolt wake length equals or exceeds bolt pitch. This may occur through a combination of high rate of rotation, low throughflow, large bolt diameter, or close pitching, but is usually precluded in real engines by practical considerations such as disc stress resulting from closely spaced bolt fixing holes. The mechanism may be understood by considering the extreme case of a disc with a continuous ring of cross section similar to a given set of discrete protrusions. Plain disc-like moment coefficients were found by Millward and Robinson for such geometry.

A correlation was found for the moment coefficient with the number and size of the bolt (expressed as the bolt diameter circumferential pitch ratio D/p). This is given by:

$$C_m = 12.2\,Re_\phi^{-0.67} C_w^{0.44} (D/p)^{0.27} \qquad (12)$$

The limits of this correlation are: hexagonal bolts; $0.17 \times 10^7 \le Re_\phi \le 1.5 \times 10^7$; $0.24 \times 10^5 \le C_w \le 1.06 \times 10^5$ and $0.024 \le (D/p) \le 0.230$. Figure 7 shows a comparison between the measured values of moment coefficient and those predicted by Equation (12). There is generally good agreement between the measured and the correlated data, particularly for $C_m < 0.02$, which is for lower values of λ_T, and those closer to engine conditions. However, for $C_m > 0.02$, the agreement is not as good. As previously noted, these data points occur at the lowest disc speeds where $\omega < 3000$ rev/min. The measured torque is relatively small in this region and the measurement uncertainties are relatively large.

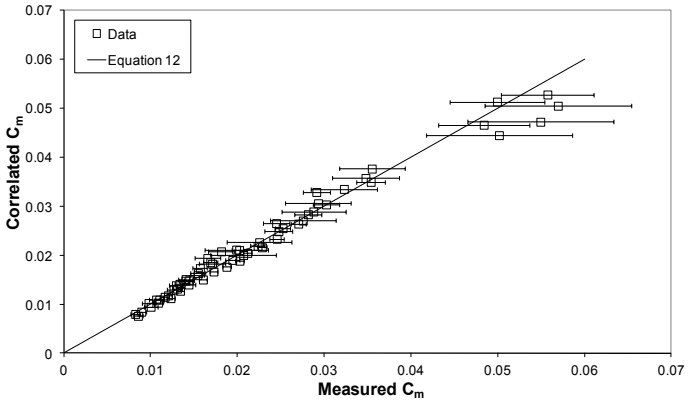

Figure 7 Hexagonal Rotor Bolts, Measured and Correlated Values of C_m.

Temperature measurements of the disc surface were made using infra red sensors at five radial locations: r = 0.096 m, 0.135 m, 0.154 m, 0.200 m and 0.211 m (r/b = 0.427, 0.600, 0.684, 0.887 and 0.935). Figure 8 shows the variation of the local disc-surface-to-inlet-air (static) temperature difference with non-dimensional radius, for N = 9, D = 10 mm, 13 mm and 16 mm, $C_w = 0.3 \times 10^5$, $Re_\phi = 10^7$ and $\lambda_T = 0.06$. Also shown is the adiabatic disc surface temperature for a free disc, $T_{0,ad} - T_\infty$ given by Owen and Rogers [4] as:

$$T_{0,ad} - T_\infty = R\,\frac{\omega^2 r^2}{2C_p} \qquad (13)$$

In this and subsequent figures, T_∞ is taken as the measured static air temperature at inlet to the cavity, T_{in}. C_p is the specific heat of the air at constant pressure. The recovery factor R was evaluated from $R = Pr^{1/3}$ where the value of the Prandtl number was taken as Pr = 0.72, and where:

$$Pr = \frac{\mu C_p}{k} \qquad (14)$$

The location of the bolt is also shown in Figure 8, by the dashed lines in the region of r/b = 0.9. The measured disc surface temperatures show a significant increase above the adiabatic disc temperature. This is attributed to the increased windage due to the presence of the bolts. This bolt windage comprises heating associated with the work done pumping the through-flowing fluid from a tangential velocity close to zero as it enters the cavity, towards that of the bolt as it exits the cavity, as well as turbulent trailing wake losses. The temperature rise is not restricted to the region in the proximity of the bolts, because of radial conduction towards the inner radius of the disc. For this reason, comparison with an adiabatic reference rather than equivalent plain disc temperature data is considered less ambiguous.

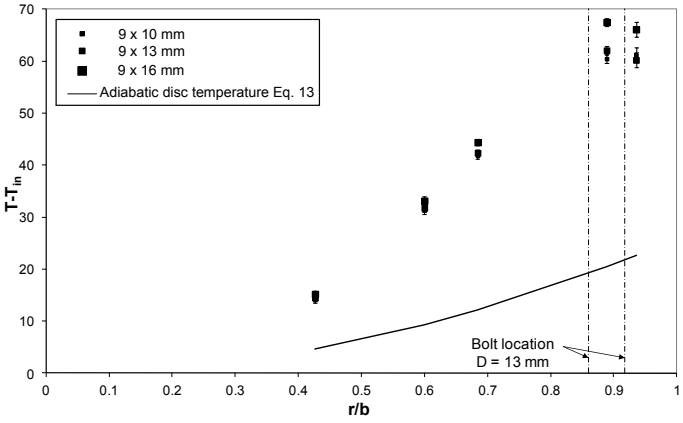

Figure 8 Hexagonal Rotor Bolts, Variation of Disc-Surface-to-Inlet-Air Temperature Difference with Non-Dimensional Radius; N = 9, D = 10 mm, 13 mm and 16 mm, $C_w = 0.3 \times 10^5$, $Re_\phi = 10^7$ and $\lambda_T = 0.06$.

The effect of bolt diameter on the measured disc surface temperature is also illustrated in Figure 8. In the region of the bolt radius, it can be clearly seen that increasing the frontal area of the bolt by increasing the diameter causes an increase in the disc surface temperature. These results were obtained at a high rotational speed and a low superimposed mass flow and as can be seen there is a relatively large rise in surface temperature and the uncertainty is small. Although not shown here, at large values of λ_T the uncertainty in the measurement of surface temperature is relatively large and it is not possible to discern a consistent effect of bolt diameter on the measured value of disc surface temperature.

An average disc surface to air inlet temperature difference may be obtained from:

$$T_{ave} = \frac{2}{r_5^2 - r_1^2} \int_{r_1}^{r_5} T\, r\, dr \qquad (15)$$

where $r_1 = 0.096$ m and $r_5 = 0.211$ m, are the radial locations of the inner and outer infra red sensors. The integral in Equation (15) was calculated using Simpson's Rule. As the infra red sensors are not evenly spaced over the radius of the disc, a third order polynomial was fitted to the data and the disc temperature obtained at five equidistant points ranging for $r_1 \le r \le r_5$. Figure 9 shows the effect of increasing the number of bolts on the average disc-surface-to-air-inlet temperature rise for a range of nominally constant values of λ_T. For reference, plain disc measurements are also indicated on the left hand vertical axis.

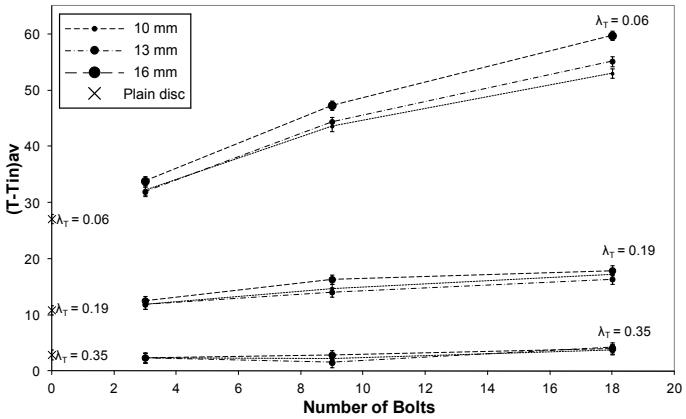

Figure 9 Hexagonal Rotor Bolts, Variation of Average Disc-Surface-to-Inlet-Air Temperature Difference with N for a Range of Nominally Constant λ_T; N = 3, 9, 18, and D = 10 mm, 13 mm and 16 mm.

Considering first the data points for $\lambda_T = 0.06$, a clear trend of increasing temperature difference with number and diameter can be seen. In this case, the temperature rise at these conditions is significantly above the uncertainty level of the measurements. For $\lambda_T \ge 0.09$, the variations in surface temperature with bolt diameter are of a similar order to the measurement uncertainty. Consequently, clear trends in the temperature data at these conditions are not to be expected with the instrumentation used. For $\lambda_T \le 0.19$, there is a consistent increase in the measured average disc surface temperature with N. This is not shown at the largest value of λ_T because of the large relative uncertainty in the measurement of surface temperature.

A comparison is made between the D = 13 mm hexagonal and bi-hexagonal (12 sided) bolt forms in Figure 10 for $\lambda_T = 0.06$, 0.019 and 0.35. For N = 0, the symbols give the measured values from the plain disc tests. As previously noted, at large values of Re_ϕ (i.e. small λ_T) the uncertainty in the torque measurement is relatively small. In general, the results show that the bi-hexagonal bolts require less torque than the hexagonal bolts. This effect is consistent with a reduction in drag coefficient that would be expected from the bi-hexagonal bolt form. Although not presented here, the differences in average disc temperature between the two bolt forms are consistent with the moment coefficient measurements. Comparing the magnitude of the plain disc results shown here with that for the bolts, shows that for N ≥ 9, form drag is expected to dominate the overall windage. Consequently, for N = 3, any difference in moment coefficient between the hexagonal and bi-hexagonal bolts is to be expected to be lost in the uncertainty of the measurement.

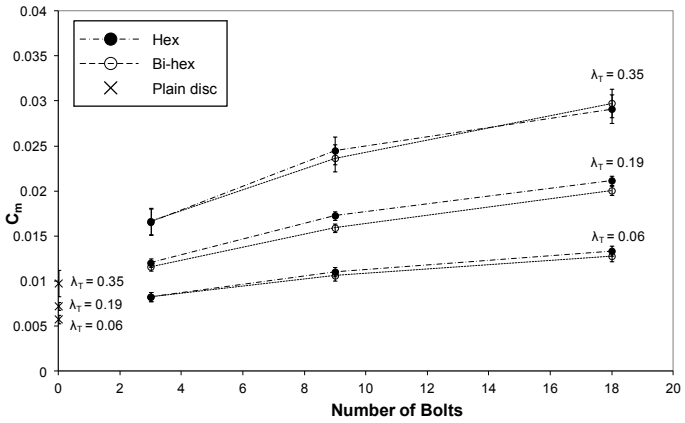

Figure 10 Variation of Moment Coefficient with Number of Bolts, N, for both Hexagonal and Bi-Hexagonal Bolts.

To investigate the effect of rotor-mounted pockets, an insert was made with a recess of 10 mm diameter and 6 mm depth. As with the rotor bolts, these pockets were attached to both sides of the disc and 3, 9 and 18 pockets were tested. The results are consolidated in Figure 11 which shows the variation of $C_m\,Re_\phi^{0.2}$ with λ_T for the pockets, together with the data for D = 10 mm bolts.

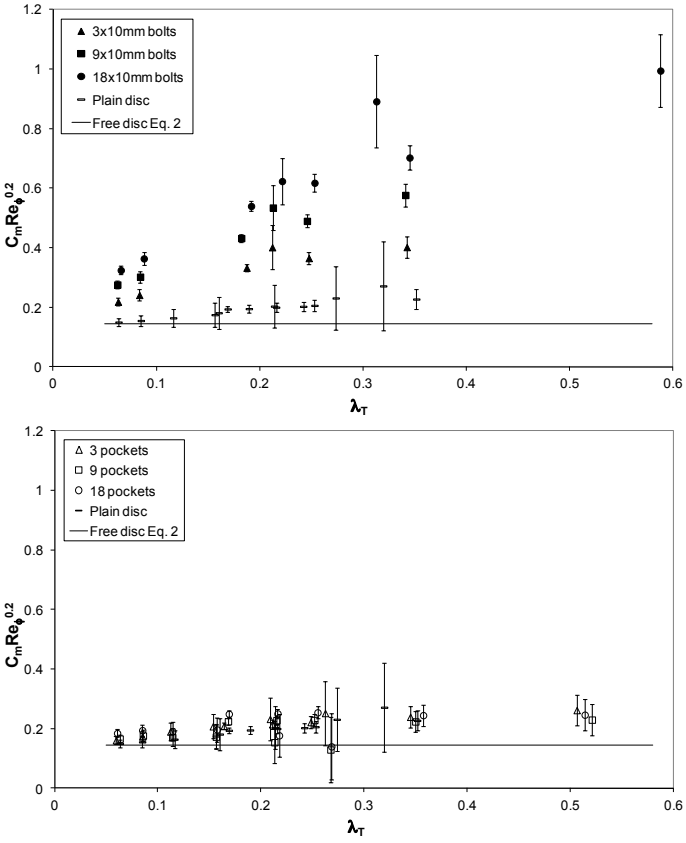

Figure 11 Variation of $C_m\,Re_\phi^{0.2}$ with λ_T for Tests with N = 3, 9 and 18 Pockets and D = 10 mm, N = 3, 9 and 18 Bolts.

As can be seen, within the bounds of experimental uncertainty there does not appear to be any discernible difference between the results for the rotor with 10 mm pockets and those for the plain disc. Nor does there seem any noticeable effect of the number of pockets on the measured values of moment coefficient. This is considered to be due to the small size which is insufficient to support any recirculation in the flow that could make a noticeable difference to the moment coefficient.

5. CONCLUSIONS

A pressurised rotor-stator test rig has been used to investigate the phenomenon of windage at a range of non-dimensional conditions which include engine-representative values. Tests were carried out with hexagonal and bi-hexagonal (12 sided) rotor bolts and a single design of rotor pocket. Three different diameters were investigated for the hexagonal bolts: D = 10 mm, 13 mm and 16 mm and a single diameter, D = 13 mm, for the bi-hexagonal bolts. In both cases (and also for the pockets) the number of bolts was discretely varied as N = 3, 9 and 18. The tests covered the following range of non-dimensional variables: $0.17 \times 10^7 \le Re_\phi \le 1.68 \times 10^7$; $0.24 \times 10^5 \le C_w \le 1.06 \times 10^5$; $0.058 \le \lambda_T \le 0.631$. Measurements were made of the rotor torque and surface temperature. The conclusions are summarised below:

- The results show that increasing the number of bolts increases the moment coefficient and windage heating. At values of λ_T considered to be representative of conditions inside an engine cavity ($\lambda_T \sim 0.06$), the uncertainties in the measured data are relatively small and the effects on windage torque and heating are clearly seen in the measurements.
- Increasing the diameter of the bolts is less conclusive, but when uncertainties in the data are taken into consideration there appears to be a consistent overall increase from the D = 10 mm to the larger D = 16 mm bolts. This is attributed to an increase in form drag which is expected to dominate the moment coefficient and windage heating at most of the conditions tested. The variation of drag coefficient for a cylindrical form in pure cross flow suggests that the change in diameter from 10 mm to 13 mm to 16 mm at some non-dimensional conditions would cover the transition from laminar to turbulent separation with an associated reduction of drag coefficient from approximately 1.0 to 0.2. So, changes in form drag from the protrusions are not necessarily expected to be directly proportional to diameter.
- For hexagonal bolts, a correlation for the moment coefficient, C_m, the diameter to circumferential pitch, D/p, and dimensionless flow parameters, Re_ϕ and C_w, and which is considered to be more appropriate than equation 9 for cases where $Re_\phi \ge 10^6$, was found to be:

$$C_m = 12.2\ Re_\phi^{-0.67}\ C_w^{0.44}\ (D/p)^{0.27}$$

- The use of bi-hexagonal (12 sided) as opposed to hexagonal bolts appears to reduce drag and windage heating and this is consistent with a reduction in drag coefficient from the bi-hexagonal bolt form.
- The introduction of pockets onto the disc has little effect on either windage heating or moment coefficient, this is attributed to the relatively small size of pockets used.

ACKNOWLEDGMENTS

The authors of this paper wish to acknowledge the support of Rolls-Royce plc who funded this work.

REFERENCES

[1] Dorfman, L. A., 1963, "Hydrodynamic Resistance and the Heat Loss of Rotating Solids", Edinburgh, Oliver & Boyd, ISBN -10:0-0500-0837-4.

[2] von Kármán, T., 1921, "Technical Memorandum on Laminar and Turbulent Friction", National advisory committee for aeronautics, Report No. 1092.

[3] Daily, J.W., Nece, R.E., 1960, "Chamber Dimension Effects on Induced Flow and Frictional Resistance of Enclosed Rotating Discs", Journal of basic engineering, Vol.82., pp.217-232.

[4] Owen, J. M., Rogers, R. H., 1989, "Flow and Heat Transfer in Rotating-Disc Systems." Volume one – Rotor-Stator Systems, Research Studies Press Ltd., ISBN 0 86380 090 4. p.101

[5] Daily, J. W., Ernst, W. D. and Asbedian, V., 1964, "Enclosed Rotating Discs with Superposed Throughflow", Dept. of Civil Engineering, MIT, Report No. 64.

[6] Millward, J. A. and Robinson, P. H., 1989, "Experimental Investigation into the Effects of Rotating and Static Bolts on Both Windage Heating and Local Heat Transfer Coefficients in a Rotor-Stator Cavity.".ASME Gas Turbine and Aeroengine Congress and Exposition, Paper No. 89-GT-196.

[7] Zimmerman, H., Firsching, A., Dibelius, G. H., and Ziemann, M., 1986, "Friction Losses and Flow Distribution for Rotating Discs with Shielded and Protruding Bolts.", ASME Gas Turbine and Aeroengine Congress and Exposition, Paper No. 86-GT-158.

[8] Gartner, W., 1997, "A Prediction Method for the Frictional Torque of a Rotating Disc in a Stationary Housing with a Superimposed Radial Outflow", ASME Gas Turbine and Aeroengine Congress and Exposition, Paper No. 97-GT-204.

[9] Gartner, W. 1998, "A Momentum Integral Method to Predict the Frictional Torque of a Rotating Disc with Protruding Bolts", ASME Gas Turbine and Aeroengine Congress and Exposition, Paper No. 98-GT-138.

[10] Miles, A., Childs, P., Long, C., 2008, "Progress Report on Turbine Disc Bolt Windage Experimental Work", Thermo-Fluid Mechanics Research Centre technical report 08/TFMRC/TR277.

[11] Coren, D., 2007, "Windage due to Protrusions in Rotor-Stator Systems", Thermo-Fluid Mechanics Research Centre, University of Sussex, D.Phil. thesis.

[12] Kurokawa, J, Toyokura, T, Shinjo, M, Matsuo, K., 1978, "Roughness Effects on the Flow along an Enclosed Rotating Disk", Bulletin of the JSME, Vol. 21, No. 162.

[13] Schlichting, H., 1979, "Boundary-Layer Theory", McGraw-Hill Book Company.